Math Geosci (2013) 45:49–68
DOI 10.1007/s11004-012-9427-0

A Spectral Analysis Based Methodology to Detect Climatological Influences on Daily Urban Water Demand

Jan Adamowski · Kaz Adamowski · Andreas Prokoph

Received: 2 April 2012 / Accepted: 3 October 2012 / Published online: 19 October 2012

Abstract Urban water demand (UWD) is highly dependent on interacting natural and socio-economic factors, and thus a wide range of data analysis and forecasting methods are required to fully understand the issue. This study applies, for the first time, the continuous wavelet transform to determine changes in the temporal pattern of UWD and its potential meteorological drivers for three major Canadian cities: Calgary, Montreal, and Ottawa. This analysis is complemented by Fourier and cross-spectral analysis to determine inter-relationships and the significance of the patterns detected. The results show that the annual (365 days) cycle provides the most consistent and significant relationship between UWD and meteorological drivers. Wavelet analysis shows that UWD is only sensitive to air temperature in the summer months when mean daily temperatures are greater than 10 to 12 °C. For the three cities studied, the UWD increases by between 10 ML (Montreal) and 50 ML (Calgary) per day with every 1 °C increase in air temperature. In an area with low precipitation (Calgary), there is an inverse relationship between UWD and precipitation during summer months. Wavelet transform and Fourier analysis also detected a 7-day cycle in UWD, particularly in the more industrialized city of Montreal, which is related to the working week. In general, applying the season dependent linear relationships between UWD and temperature is suggested as perhaps being more appropriate and potentially successful for forecasting, rather than continuous complex nonlinear algorithms that are designed to explain variability in the entire UWD record.

J. Adamowski
Department of Bioresource Engineering, McGill University, 21 111 Lakeshore Road, Ste. Anne de Bellevue, QC, H9X 3V9, Canada

K. Adamowski
Department of Civil Engineering, University of Ottawa, Ottawa, ON, K1N 6N5, Canada

A. Prokoph (✉)
SPEEDSTAT, 19 Langstrom Crescent, Ottawa, ON, K1G 5J5, Canada
e-mail: aprokocon@aol.com

Keywords Precipitation · Air temperature · Continuous wavelet transform · Fourier analysis

1 Introduction

The need for defining the factors that influence urban water demand (UWD) has dramatically increased in recent decades as population growth, industrialization, and an increased likelihood of extreme climate events due to anthropogenic global warming lead to challenges in balancing water supply and demand (IPCC 2007). Although Canada holds approximately 7 % of the world's freshwater and only 0.5 % of the world's population (Environment Canada 2010), many of Canada's cities are experiencing some degree of water stress. This is due to a complex combination of factors, including population growth and water losses from ageing infrastructure, as well as the fact that most of the freshwater flows north away from the main areas of population (Adamowski et al. 2009). In addition, Canada is also experiencing the regional impact of global climate change, which makes future levels of supply and demand uncertain. For example, Zhang et al. (2000) highlighted that annual precipitation totals have generally increased by 5 % to 35 % across Canada between 1950 and 1998, although the most significant increases occurred north of 60° N. Despite often limited water availability and uncertain future supplies, few studies on detecting relationships between temporal patterns in UWD and meteorological records in Canada have been carried out to date (Adamowski and Karapataki 2008; Adamowski et al. 2012). While meteorological records in major Canadian cities are mostly over 50 years long, UWD records are much shorter and often incomplete. Only three cities (Calgary, Ottawa, and Montreal) in Canada have readily available recorded daily urban water demand and meteorological data simultaneously without gaps for intervals of more than five successive days. These three cities represent different climatic and economic environments, with Calgary having a continental dry climate and minor manufacturing, Ottawa having a moderately continental humid climate and minor manufacturing, and Montreal having a moderately continental humid climate and strong manufacturing industry.

Research into UWD has increased since the end of the twentieth century, with particular focus on forecasting UWD and describing the complexity of the factors that influence it (House-Peters and Chang 2011). Such factors are highly complex, but can be divided into socio-economic factors and natural factors. Socio-economic variables such as water price, rate structures, and population growth exhibit mostly nonlinear temporal patterns and are analyzed accordingly (Arbués et al. 2004, 2010). Research on the influence of natural factors on UWD has focused especially on meteorological factors that are incorporated in complex log-linear water demand models (Miaou 1990; Schleich and Hillenbrand 2009). Traditional statistical models of urban or residential demand have tended to be based on a wide range of socio-economic and natural variables, including meteorological variables such as temperature, precipitation, days of sunshine, and wind speed. Commonly used models include multiple linear regression (MLR) and auto-regressive moving average (ARIMA), which acknowledge seasonal variability in both water supply and urban demand (Anderson et al. 1980;

Maidment and Parzen 1984). For example, Agthe and Billings (1980) included a time lagged value in a multiple regression model to better account for the influence of past water use on current water use. Maidment et al. (1985) used regression analysis to model the association between daily municipal water consumption and rainfall and air temperature.

Several studies acknowledged the different UWD dependencies on seasonal sensitive (summer) weather compared to relatively non-sensitive (winter) weather by implementing a sinusoidal variability model (Gato et al. 2007; Praskievicz and Chang 2009). In addition, Zhou et al. (2000) developed a method that recognizes that seasonal variations in water consumption are not completely the result of cyclic patterns of air temperature and evaporation over a year, but are also related to abrupt and extreme events, such as floods and drought. Moreover, short-time extreme precipitation events that lead to rapid UWD reductions cannot be reconstructed or modeled using sinusoidal models or Fourier analysis. Thus, auto-regressive methods with short-term memory functions have been developed to address the relationships between meteorological events and UWD changes (Agthe and Billings 1980; Zhou et al. 2000).

Maidment and Miaou (1986) demonstrated that models assuming linear relationships between weather variables and water demand are not adequate. For example, it has been suggested that water use responds to the occurrence of rainfall rather than the amount that falls (Martínez-Espiñeira 2002). Furthermore, it is likely that there are thresholds in temperature and/or precipitation, above which water demand changes. For example, Gato et al. (2007) identified thresholds that separate the base water use, which is independent of temperature and rainfall, from seasonal water use. A further drawback of many of the statistical models of UWD and meteorological factors described above is that they are based on an assumption of stationarity in data.

The wavelet transform (WT) is an alternative method that has not previously been used for detecting relationships between temporal patterns in UWD and meteorological records. In contrast to MLR, ARIMA, ANN, or Fourier analysis used for UWD and meteorological records (House-Peters and Chang 2011, and references therein), WT permits the detection of temporal patterns synchronously according to their scale (or frequency/wavelength) at varying temporal resolutions (Rioul and Vetterli 1991). Therefore, signals can be extracted according to their scale as well as their time of occurrence, meaning for example that UWD cycles restricted to a certain season, as well as short-term stochastic events such as precipitation, can be identified. Continuous WT (CWT) permits signal detection at a very wide range of bandwidth and temporal resolutions, in contrast to the more commonly used discrete WT (DWT) (Adamowski et al. 2012). The multi-resolution feature of the CWT leads to higher precision in defining intervals and wavelengths of significant UWD variability than Fourier analysis. Fourier and cross-spectral analysis can be used to support WT results due to their more sophisticated definitions of significance and confidence, as was done in this study.

This study aims to demonstrate the relevance of a spectral analysis based methodology that includes the continuous wavelet transform for determining temporal-frequency dependency patterns. A particular goal of this study is to compare

differences in urban water demand and meteorological/climatological factors in different climatic and economic regions of Canada.

2 Methodology

The methodology consists of:

1. The wavelet transform is used to qualitatively detect periodic sinusoidal signals according to their time intervals of occurrence, as well as their wavelengths in meteorological and corresponding UWD records for the three selected major urban centers in Canada.
2. Time intervals of the records exhibiting different cyclicity and/or variability patterns that were detected by the wavelet transform are separately analyzed for links between meteorological records and UWD records.
3. Fourier analysis is then used to quantify the significance of the detected cycles.
4. Cross-spectral analysis is applied to quantify the correlation between the time series at specific wavelengths between meteorological and UWD records.

The steps of analysis and the results are described for each location separately, in order to emphasize the procedure and location specific features. The results are then discussed in relation to specific locations.

3 Time Series Analysis Background

3.1 Wavelet Analysis

Wavelet analysis was first developed as a filtering and data compression method for geophysical exploration in the 1980s (Morlet et al. 1982). It transforms a time series into a frequency domain by simultaneously transforming the depth or time domain and the scale or frequency domain using various shapes and sizes of short filtering functions called wavelets. The CWT method allows for the automatic localization of periodic signals, gradual shifts, abrupt interruptions, trends, and onsets of trends in time series data (Rioul and Vetterli 1991). The wavelet coefficients W of a time series $x(s)$ are calculated by a simple equation

$$W_\psi(a,b) = \left(\frac{1}{\sqrt{a}}\right) \int x(s)\psi\left(\frac{s-b}{a}\right) ds, \tag{1}$$

where ψ is the mother wavelet, a is the scale factor that determines the characteristic frequency or wavelength, and b represents the shift of the wavelet over $x(s)$ (Prokoph and Barthelmes 1996).

The bandwidth resolution for a wavelet transform varies with $\Delta a = \frac{\sqrt{2}}{4\pi a l}$, and a location resolution $\Delta b = \frac{al}{\sqrt{2}}$. Due to Heisenberg's uncertainty principle $\Delta a \Delta b \geq 1/4\pi$, the resolution of Δb and Δa cannot be arbitrarily small (Prokoph and Barthelmes 1996). Parameter l is used to modify the wavelet transform bandwidth resolution either in favor of time or in favor of frequency.

In this study, the CWT was used with the Morlet wavelet as the mother function (Morlet et al. 1982), which is expressed as

$$\psi(s) = \pi^{-\frac{1}{4}} e^{-i2\pi f_0 s} e^{-\frac{s^2}{2}}. \tag{2}$$

The Morlet wavelet is a sinusoid with wavelength/scale a modulated by a Gaussian function (Torrence and Compo 1998; Adamowski et al. 2009). The Morlet wavelet has been widely and successfully used on hydrological and meteorological records (Ware and Thomson 2000; Coulibaly 2006). The matrix of the wavelet coefficients $W_l(a, b)$, the so-called 'scalogram', was coded in a color scale (orange highest, blue lowest $W_l(a, b)$), for better graphical interpretation. Edge effects of the wavelet coefficients occur at the beginning and end of the analyzed time-series and increase with increasing wavelength (scale) and parameter l. Thus, a 'cone of influence of edge effects' is formed (Torrence and Compo 1998). The cones of edge effect influences of greater than 10 % of bias due to non-available data points in the analysis windows behind the edges are illustrated in the scalograms.

The wavelet coefficients W are normalized by using the L1 normalization $(1/a)$, replacing the commonly used $1/\sqrt{a}$ L2 or L^2 normalization (see Eq. 1). This allows wavelet coefficients to be interpreted in terms of Fourier amplitudes (Prokoph and Barthelmes 1996). In addition, the L2 normalization of the Morlet wavelet commonly leads to overvaluing wavelet coefficients in long wavelengths compared to shorter ones, as discussed in detail by Schaefli et al. (2007). Detailed explanations of the advantages and disadvantages of the normalization types, in terms of accuracy of the energy spectrum, amplitudes and white noise, variance and bias of arbitrary estimated continuous wavelet spectra depending on the algorithms applied are provided by Maraun and Kurths (2004) and Maraun et al. (2007). The parameter $l = 6$ was chosen for all analyses as it provides sufficiently precise results in the resolution of time and scale, and is commonly suggested for hydrological and meteorological records (Schaefli et al. 2007; Adamowski et al. 2009). Significance tests for the WT were not included in this study since the significance tests for WT, as for example suggested by Torrence and Compo (1998), are based on the assumption of combined white and red-noise for windows of discrete scales (frequency)–location (time-intervals), but have not been proven to correctly evaluate the significance of signals of deterministically changing frequencies and amplitude (so-called "chirps"). For this reason, this study applied significance tests on Fourier analysis for time-intervals proven (by WT) to have approximately stationary signals since this was deemed to be better suited for this research.

The wavelet analysis technique used in this article is explained in detail in Prokoph and Barthelmes (1996) and Adamowski et al. (2009).

3.2 Fourier Analysis

Fourier transform (Fourier analysis) is defined by

$$P_f = \int x(t) e^{i2\pi f t}\, dt \quad t = 1 \ldots N, \tag{3}$$

with $x(t)$ as the discrete time series, f the frequency, and P as the spectral power (Davis 2002). The white noise level P_w and the red noise level were calculated

from the lag-one auto-correlation coefficient r according to an auto-regressive model (Mann and Lees 1996), using a χ^2 value for the chosen confidence level (95 %) at 1 degree of freedom. The value of B_f is the Fourier power of the background spectrum for the Fourier frequencies k combining the red and white noise spectrum and the confidence level set by the χ^2 value. The Fourier power P_w of a white noise spectrum is equal to the average power of all frequencies f

$$B_f = P_w \chi^2 \frac{1 - r^2}{1 + r^2 - 2r\cos(2\pi f/N)}. \tag{4}$$

Only frequencies (or wavelengths) where $P_f^2 > B_f$ for confidence levels greater than 95 % were considered to be significant in this study. Fourier analysis and confidence level calculations were carried out using the REDFIT software (Schulz and Mudelsee 2002).

3.3 Cross-spectral Analysis

Cross-spectral analysis is an extension of Fourier analysis for two time series (Bassett and Tinline 1970). The cross spectrum S_{yz} of two time-series y and z with power spectra S_{yz} and S_{yz}, respectively, is defined by

$$S_{yz}(f) = dS_{yy}(2\pi f) dS_{zz}^*(2\pi f). \tag{5}$$

It should be noted that the cross spectrum is a complex variable with a real and an imaginary component

$$S_{yz}(f) = Co(2\pi f) + iQuad(2\pi f), \tag{6}$$

where Co is the co-spectrum (in-phase covariance), which constitutes the real component, and $Quad$ is the quadrature spectrum (out-off-phase covariance), which constitutes the imaginary component. The cross spectrum can be normalized to obtain the spectral equivalent of the correlation coefficient, the coherency spectrum

$$R_{yz}(f) = \frac{|S_{yz}(f)|}{S_{yy}(f) S_{zz}(f)}. \tag{7}$$

The coherency spectrum can be tested for confidence in a similar way to the correlation coefficient. As for the spectral estimate, the numerical solution reflects that the time-series is finite using N equally spaced locations. The cross spectrum provides the density of covariance between two variables (y, z) in the Fourier domain (the frequency of the sine and cosine wave domain)

$$S_{yz}(f_k) = \frac{1}{M} \sum_{i=1}^{M} \left\{ \frac{2\Delta x}{(2m+1)N^2} \sum_{l=-m}^{m} C_{iyz}(f_{k+l}) + \iota Q_{iyz}(f_{k+l}) \right\}, \tag{8}$$

with

$$C_{iyz}(f_k) = A_{iy} A_{iz} + B_{iy} B_{iz}, \tag{9}$$

and

$$Q_{iyz}(f_k) = A_{iz} B_{iy} - A_{iy} B_{iz}, \tag{10}$$

Fig. 1 Map of Canada with survey locations

with the real component (*co-spectrum*) for M averaged transects

$$C_{yz}(f_k) = \frac{1}{M}\sum_{i=1}^{M}\left\{\frac{2\Delta x}{(2m+1)N^2}\sum_{l=-m}^{m} C_{iyz}(f_{k+l})\right\}, \tag{11}$$

and the imaginary component (*quadrature spectrum*)

$$Q_{yy}(f_k) = \frac{1}{M}\sum_{i=1}^{M}\left\{\frac{2\Delta x}{(2m+1)N^2}\sum_{l=-m}^{m} Q_{iyz}(f_{k+l})\right\}. \tag{12}$$

The squared coherency spectrum is calculated by

$$R^2_{yz}(f) = \frac{C^2+Q^2}{S_{yy}(f)S_{zz}(f)} = \frac{|S_{yz}(f)|^2}{S_{yy}(f)S_{zz}(f)}. \tag{13}$$

Here, we used a 3-spectral-estimate window for smoothing (Patterson et al. 2004). According to Jenkins and Watts (1968), the squared coherency can be tested for two variables by using the F-test:

$$F_{crit} = \frac{R^2_{yz}(f)}{1-R^2_{yz}(f)}\big((2M(2m+1)-4)/4\big). \tag{14}$$

4 Data and Study Site

The proposed WT approach was tested on three large Canadian cities, Calgary, Montreal, and Ottawa (Fig. 1) that each has more than 700,000 inhabitants, but have different climatic and socio-economic characteristics.

Calgary has a continental climate characterized by cold winters, occasionally interrupted by milder phases, and warm summers. Its climate is generally dry, although it experiences intermittent high precipitation events, such as thunderstorms or blizzards (Environment Canada 2012). Calgary is a major administrative center of the oil industry, but has no significant manufacturing industry. Residential water use is

approximately 257 liters per person per day and accounts for 52 % of the city's water consumption (City of Calgary 2012).

Both Ottawa and Montreal are located in the Saint Lawrence lowlands, which have a moderate continental climate with cold winters and humid, hot summers (Environment Canada 2012). In Ottawa, water consumption was 291 liters per person per day in 2009, which represents a decrease of 9 % since 2007, following implementation of the city's Water Efficiency Strategy (City of Ottawa 2010). The City of Montreal supplies drinking water to 1.8 million people and produces 1300 liters per person per day (Aubertin et al. 2002). The almost five times higher supply in Montreal compared to Ottawa and Calgary is due to a combination of industrial demand and securing supply for extreme peak periods. In addition, approximately 40 % of Montreal's water supply is lost in the piping due to the poor condition of the water supply piping infrastructure in the city of Montreal; this also contributes to the much higher supply that is produced in Montreal compared to Ottawa.

Daily UWD data (consumption in ML/day) for the entire municipal areas of Montreal, Ottawa and Calgary were recorded discontinuously for the last ~ 50 years for each city. For this study, a string of continuous and almost complete UWD and meteorological records of at least 1,000 days were used for each location. For the same period, mean daily air temperature and total precipitation data for the city centers were obtained from Environment Canada (Environment Canada 2012). The records include very few missing data points for less than five successive days. The gaps that did exist were addressed via linear interpolation.

For the Fourier and cross-spectral analysis, a 730-day subset (January 1st to December 31st of the following year) of the data from each location were analyzed to allow for maximum compatibility of the significance test for the same frequencies in UWD and meteorological records.

5 Results

The UWD and meteorological records for Calgary ranged from March 2004 to December 2006, thus encompassing three complete summer seasons and two complete winter seasons (Fig. 2). During all three summer seasons, mean air temperatures were greater than 10 °C (dotted line in Fig. 2B), and the UWD was often greater than 600 ML/day (Fig. 2C), particularly during successive weeks of daily precipitation that were smaller than 2 mm/day as in the summer of 2006 (Fig. 2A). The most significant variations in UWD occurred during the summer and coincided with large precipitation events. In contrast, both the data (Figs. 2A–2C) and the wavelet analysis (Figs. 2D–2F) showed that the highest temperature variability occurred during winter, while the mean summer temperatures were relatively stable at around 20 °C. All records formed an annual (~ 365 day) cycle, with the highest temperature, precipitation and UWD values occurring during the summer months.

The WT analysis highlighted cycles of approximately 25 days during the summer season (three cycles per season) in both UWD and precipitation, indicating that rainfall waves reduced the UWD, and dry periods led to increases in UWD (Figs. 2A and 2C). However, the air temperature record did not show any consistent cyclical

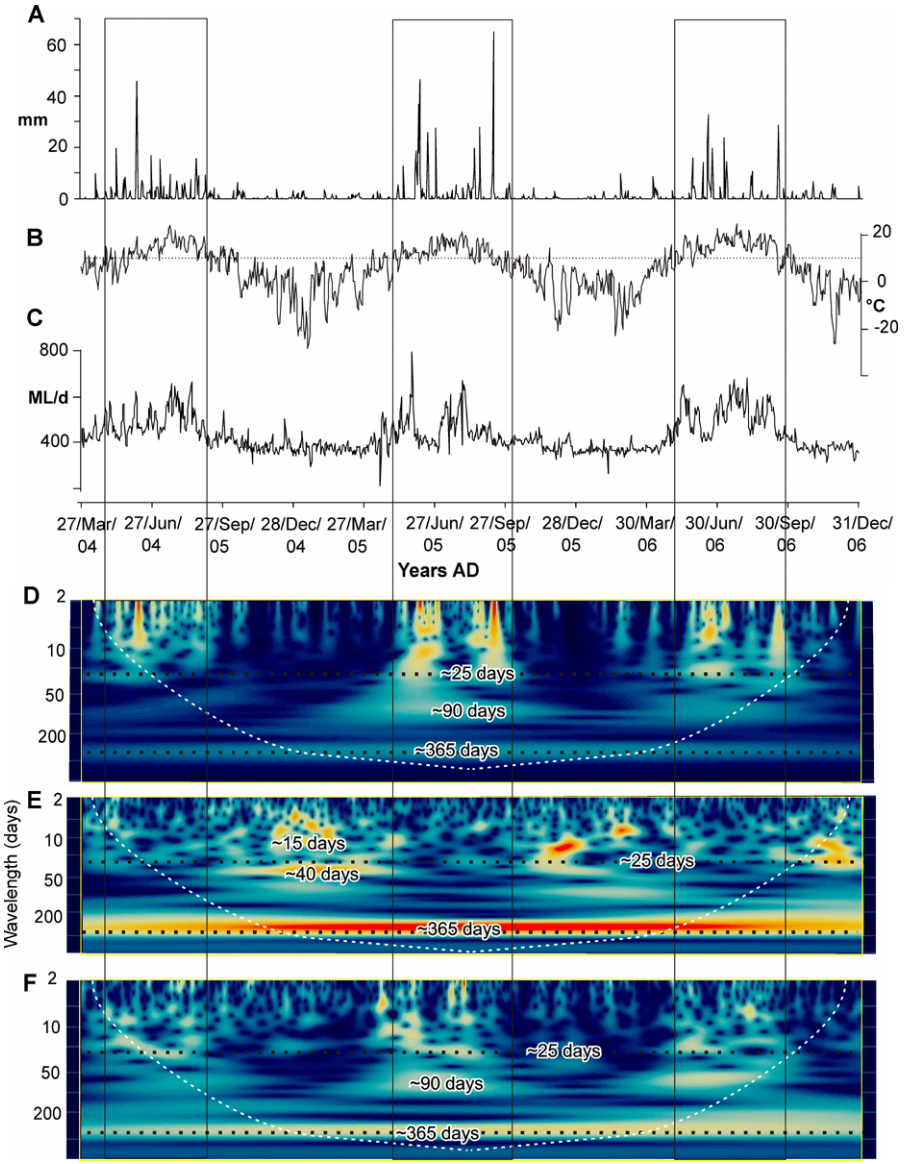

Fig. 2 Wavelet analysis of daily UWD and meteorological data from Calgary from 3/2004 to 12/2006: **A** daily total precipitation (mm); **B** daily mean temperature (°C) with sensitivity threshold (*dashed line*); **C** urban water demand (ML/d); **D** wavelet scalogram of daily total precipitation record; **E** wavelet scalogram of daily mean temperature record; **F** wavelet scalogram of daily urban water demand. *Curved dashed lines* mark "cone of influence" (see text), *horizontal dotted lines* mark 25-days scale, and *boxes* mark high UWD variability intervals. *Orange colors* indicate large wavelet coefficients and *blue colors* weak wavelet coefficients

pattern besides the annual cycle, except intermittent but strong fluctuations in a 14–40-day range during the winter and spring (Fig. 2E).

The UWD and meteorological records for Ottawa ranged from April 2006 to June 2009, spanning three complete summer and winter seasons (Fig. 3). During the summer period (May to September), the UWD was mostly greater than 350 ML/day, except after occasional periods of heavy rain (Figs. 3A and 3C). Periods of higher variability in UWD correlated with mean air temperatures of greater than 12 °C (Figs. 3E and 3F). In contrast to Calgary, the precipitation was much more evenly distributed through the year, and periods of more than two weeks during which there was no or little precipitation were almost absent (Fig. 3A). WT showed that the annual cycle ($\sim$ 365 days) dominated the air temperature and UWD pattern, superimposed by weaker 10–40 day cycles, predominately during the summer months.

In Montreal, the UWD and meteorological records ranged from February 1999 to June 2002 and encompassed three complete summer seasons and three complete winter seasons. The UWD was highest between May and September when mean daily temperature was mostly above 12 °C (Figs. 4B and 4C). Drought periods, as indicated by "white" (no signal) areas in the high-frequency field ($<$ 10 days wavelength), occurred occasionally during the summer (Fig. 4D) and were associated with increased UWD. The UWD and air temperature records were dominated by the annual cycle (Fig. 4). This is a similar pattern to that which occurred in Ottawa, which is only 180 km from Montreal and has a similar climate. In addition, the UWD and total precipitation both have 180-day and $\sim$ 50-day cycles in common, particularly during the summer months (Figs. 4D and 4F). WT also showed that the UWD is dominated by 7-day cycles related to the working week. However, during the summer this cycle was offset and vanished if large precipitation fluctuations occurred (Figs. 4A, 4C, and 4F).

Scatter plots for all three cities showed that there was no obvious relationship between daily UWD and mean daily temperature below a mean daily temperature of approximately 10 °C for Calgary, and approximately 12 °C for Ottawa and Montreal (Figs. 5A–5C). Above these temperature thresholds, the linear correlation between UWD and mean daily temperature became more than 99 % significant ($p < 0.001$) (Table 1). This confirms the pattern depicted by the wavelet analysis (Figs. 2, 3, and 4). Table 2 shows that the variability in the UWD pattern exponentially increases to temperature in all cities when the temperature thresholds of 12 °C, 10 °C, and 12 °C for Ottawa, Calgary, and Montreal are crossed, respectively. In contrast, the precipitation variability increases approximately linearly with mean daily temperature increases (Table 2).

The UWD was most strongly associated with air temperature in Calgary, where UWD increased by approximately 100 ML per day with a 2 °C increase in air temperature. While the correlation between UWD and air temperature was most significant for Montreal, an increase of approximately 100 ML per day in UWD required an increase in air temperature of approximately 10 °C (Table 1). By contrast, no relationship was found between daily records of UWD and total precipitation for any of the cities (Figs. 5D–5F).

Fourier analysis illustrated that the 365-day (annual) wavelength was more than 95 % significant in temperature and UWD for all cities. This indicates that UWD

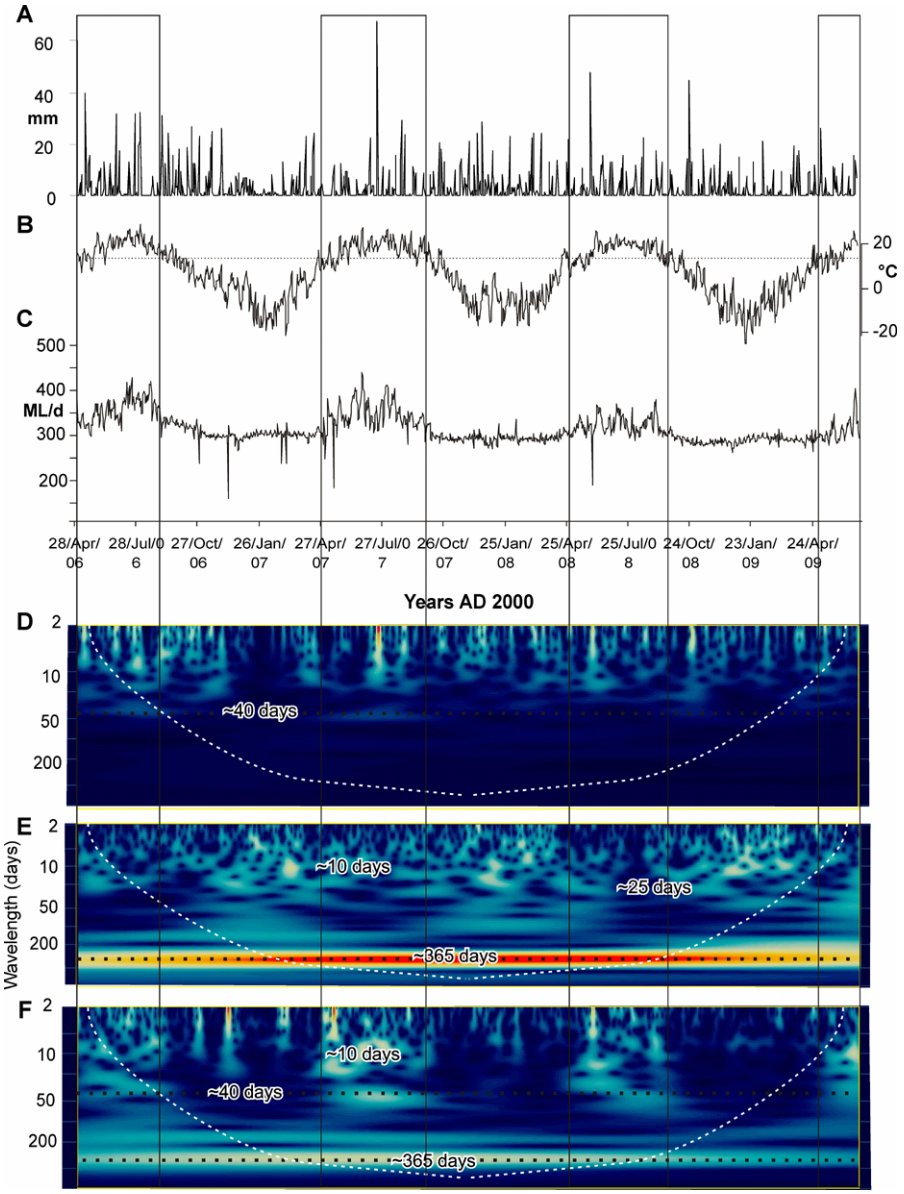

Fig. 3 Wavelet analysis of daily UWD and meteorological data from Ottawa from 4/2006 to 6/2009: **A** daily total precipitation (mm); **B** daily mean temperature (°C) with sensitivity threshold (*dashed line*); **C** urban water demand (ML/d); **D** wavelet scalogram of daily total precipitation record; **E** wavelet scalogram of daily mean temperature record; **F** wavelet scalogram of daily urban water demand. *Curved dashed lines* mark "cone of influence" (see text), *horizontal dotted lines* mark 40-days and 365-days scale, and *boxes* mark high UWD variability intervals. *Orange colors* indicate large wavelet coefficients and *blue colors* weak wavelet coefficients

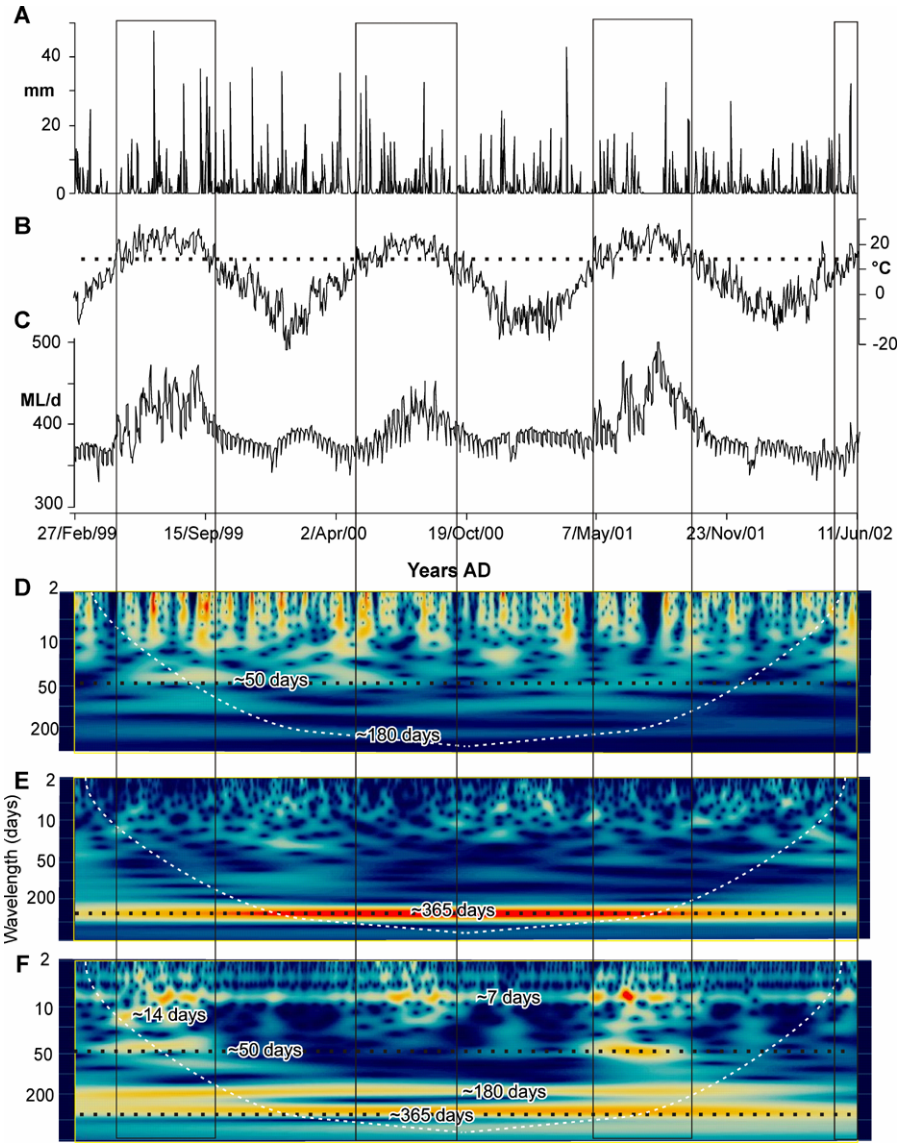

Fig. 4 Wavelet analysis of daily UWD and meteorological data from Montreal from 2/1999 to 6/2002: **A** daily total precipitation (mm); **B** daily mean temperature (°C) with sensitivity threshold (*dashed line*); **C** urban water demand (ML/d); **D** wavelet scalogram of daily total precipitation record; **E** wavelet scalogram of daily mean temperature record; **F** wavelet scalogram of daily urban water demand. *Curved dashed lines* mark "cone of influence" (see text), *horizontal dotted lines* mark 50-days and 365-days scale, and *boxes* mark high UWD variability intervals. *Orange colors* indicate large wavelet coefficients and *blue colors* weak wavelet coefficients

is strongly dependent on temperature in the three cities studied in Canada (Fig. 6). Fourier analysis also detected that the 7-day cycle related to the working week was significant for all locations, not only in Montreal as indicated by WT. The 3.5 and

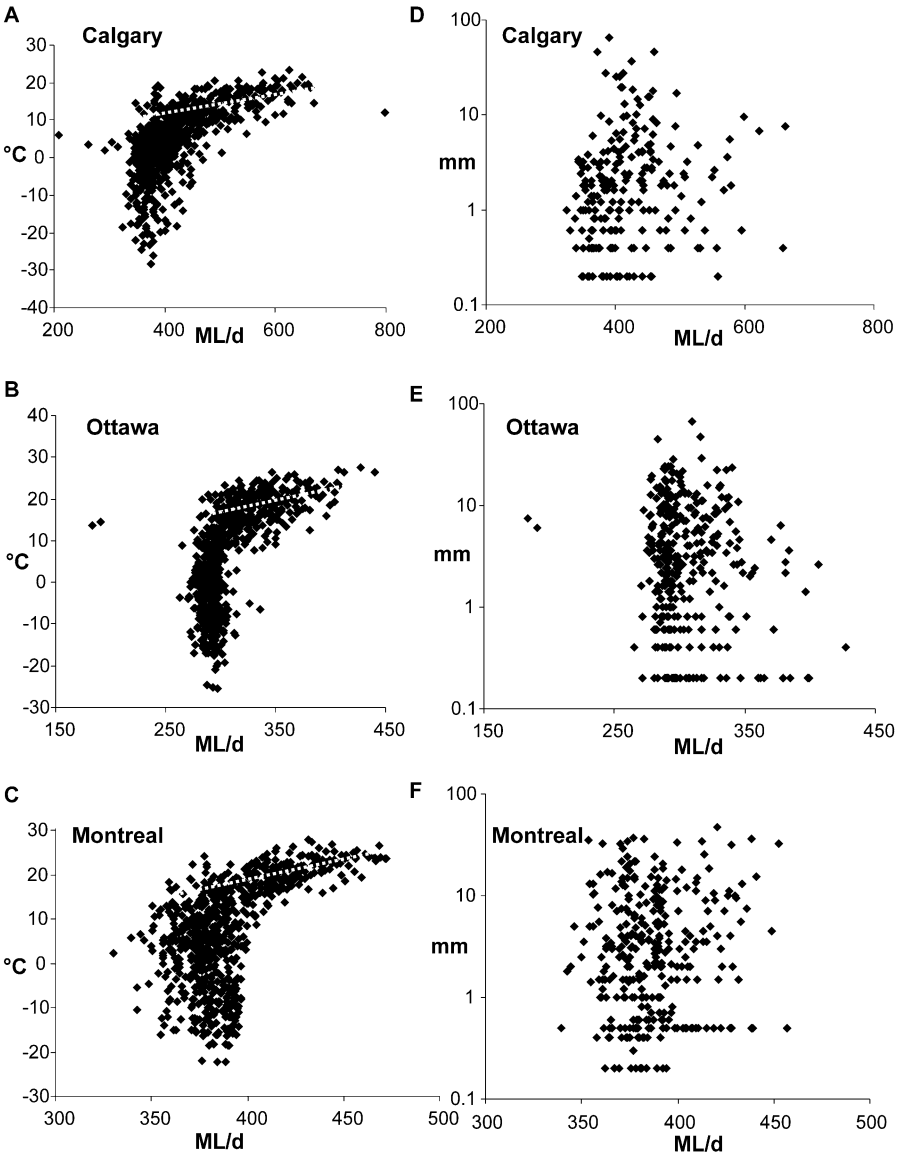

Fig. 5 Scatter plots of daily UWD versus meteorological records: **A**–**C**—UWD versus mean temperature, *dashed lines* mark regression line above temperature threshold; **D**–**F**—UWD versus total precipitation

2.3-day cycles may be harmonics (frequency-multiples) of the 7-day cycles, because the 7-day cycle is approximately step-wise (5 days work/2 days no work), and is thus not Gaussian distributed as assumed by Fourier analysis.

Cross-spectral analysis between UWD and meteorological records for the 730-day interval show potential relationships at time offsets, representing a delayed response in the Fourier domain (Fig. 7). As already evident from WT and the records

Table 1 Daily UWD–mean daily temperature relationship

	Location		
	Calgary	Ottawa	Montreal
Total number of samples	730	730	730
Temperature threshold (°C)	10	12	12
Number of samples above threshold	255	299	291
Regression equation $T = f$ (UWD)	$0.021x + 3.95$	$0.06x - 1.71$	$0.101x - 22.56$
Coefficient of determination R^2	0.28	0.26	0.49
PEARSON correlation coefficient r	0.53	0.51	0.7
Significance level p for r	< 0.001	< 0.001	< 0.001

Table 2 Mean daily temperature–daily UWD and precipitation variance relationships

	T range (°C)	UWD variance $(\text{ML/d})^2$	Precipitation variance $(\text{mm/d})^2$	% of total days
Ottawa	−24 to −6	104	16	18
	−6 to 12	246	31	39
	12 to 30	1043	45	43
Calgary	−26 to −8	496	2	8
	−8 to 10	1467	20	53
	10 to 28	5568	27	39
Montreal	−24 to −6	242	17	16
	−6 to 12	289	45	43
	12 to 30	882	54	41

themselves, there was a significant coherency between UWD and the mean temperature in the annual cycle at −0.3 to 0.16 radians, thus indicating only a minor temporal offset (Figs. 7A–7C). Similarly, a strong coherency at −0.26 radian offset also occurred between UWD and precipitation in Calgary, which highlights the correlation between the seasonal patterns of the two parameters.

There were several other significant coherencies between UWD and meteorological records in the 2.2-day to 52-day wavelength spectrum with varying phase offsets (Fig. 7). Most notably, a 7–8.5-day (weekly) cycle occurs between UWD and temperature in all locations, albeit with very different phase offsets that range from positively correlated (∼ 0.1 radians for Montreal) to inverse correlated (∼ 2.9 radians for Ottawa).

6 Discussion

This study applied CWT for the first time to determine changes in the temporal pattern of UWD and its potential meteorological drivers, specifically daily mean air temperature and precipitation, at both frequency and time-scale in three major Canadian

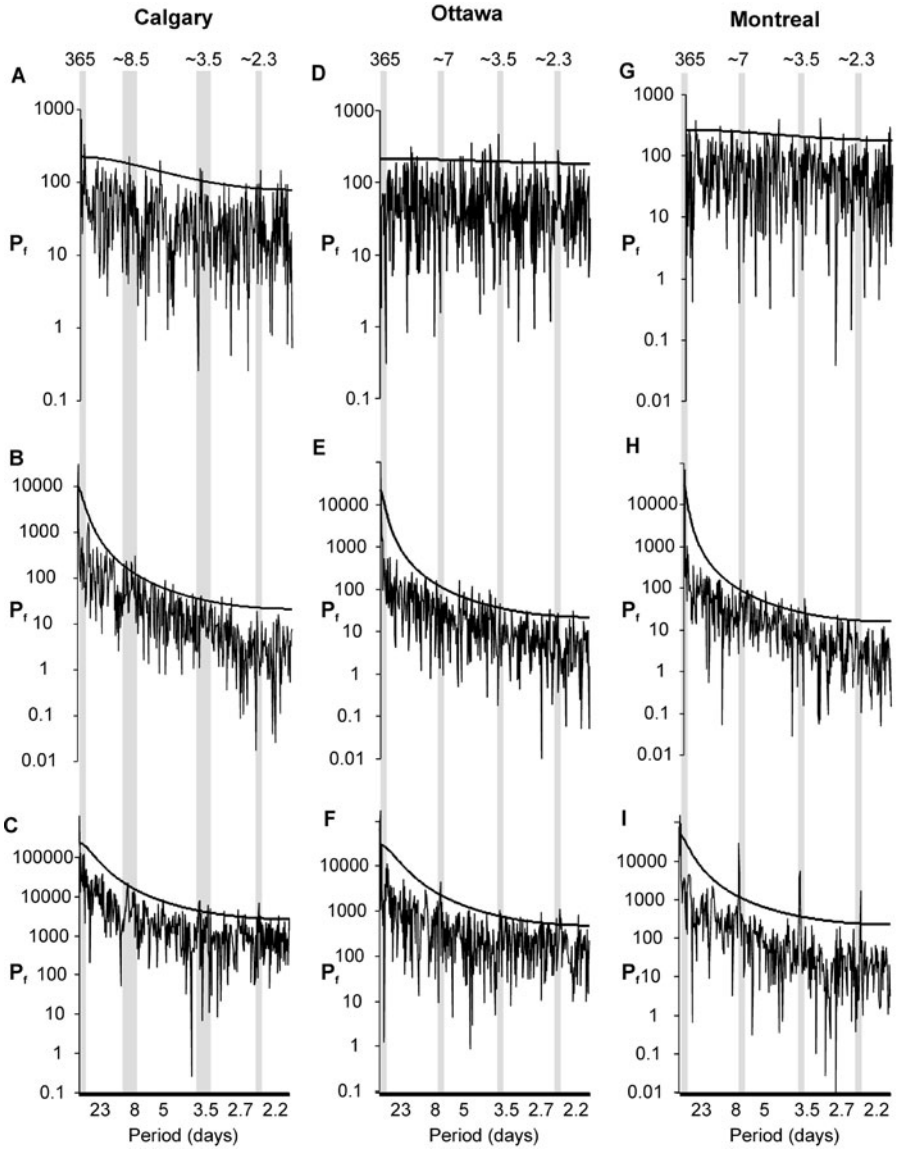

Fig. 6 Fourier analysis of daily UWD and meteorological data: **A** power spectra of daily total precipitation record from Calgary; **B** power spectra of daily mean temperature record from Calgary; **C** power spectra of daily urban water demand record from Calgary; **D** power spectra of daily total precipitation record from Ottawa; **E** power spectra of daily mean temperature record from Ottawa; **F** power spectra of daily urban water demand record from Ottawa; **G** power spectra of daily total precipitation record from Montreal; **H** power spectra of daily mean temperature record from Montreal; **I** power spectra of daily urban water demand record from Montreal. *Bold lines* mark 95 % χ^2-significance of spectral value, *vertical gray bars* highlight major wavelengths (periods)

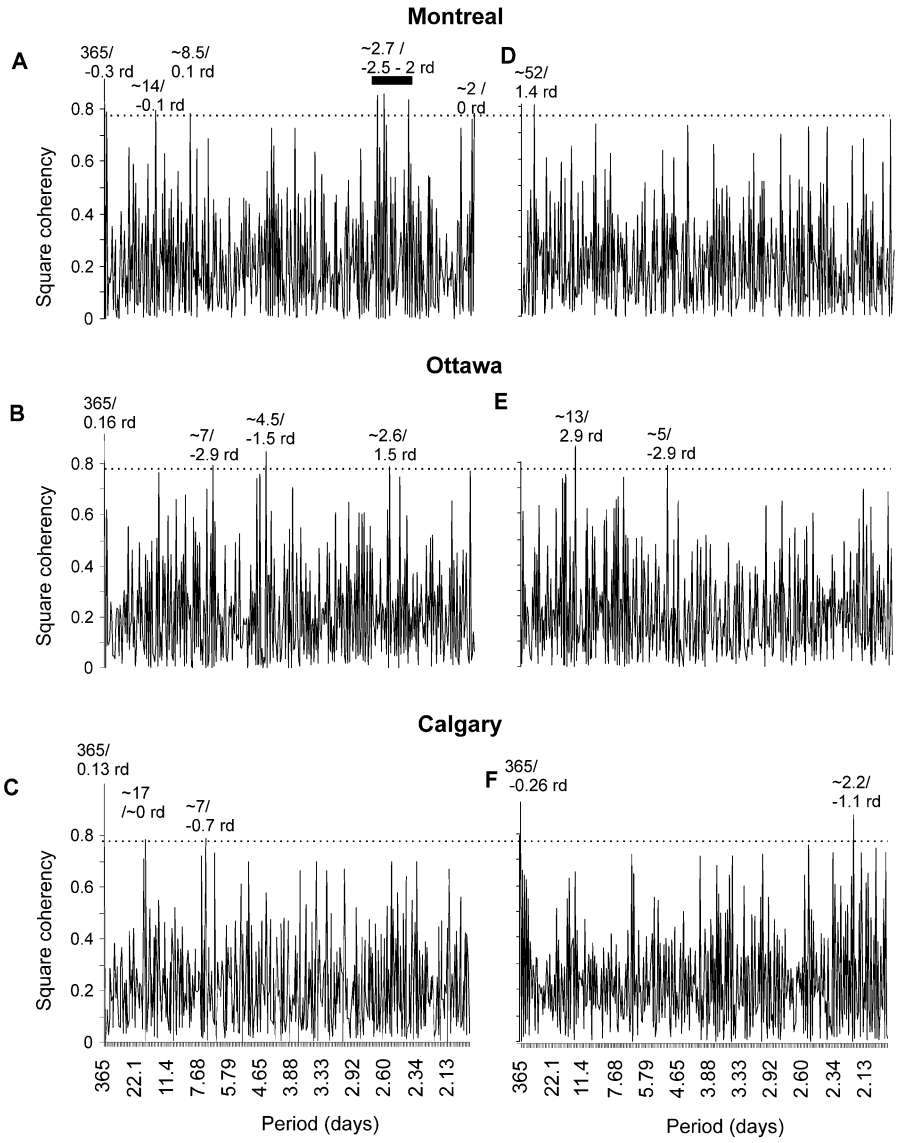

Fig. 7 Cross-spectral analysis of daily UWD versus meteorological data: **A**–**C**—UWD versus mean temperature; **D**–**F**—UWD versus total precipitation. *Dashed lines* mark squared coherencies > 0.78, squared coherencies > 0.78 are marked by *period* and phase offset in radians (rd)

cities. This analysis was aided by Fourier and cross-spectral analysis, which show that the annual (365 day) cycle provides the most consistent and significant relationship between UWD and meteorological drivers in southern Canadian cities.

The methods used detected that during the summer UWD is only sensitive to air temperature when mean daily temperatures are higher than 10–12 °C. Above this threshold, the increase in UWD for a 1 °C increase in temperature ranges from 10 ML

per day for Montreal to 50 ML per day for Calgary. In Calgary, where precipitation is lower and more seasonally distributed, the temperature relationship is amplified by the inverse UWD-precipitation relationship that occurs during the summer months. Such temperature threshold dependent UWD variability has been determined by other data analysis methods previously (Gato et al. 2007). However, the wavelet transform simultaneously provides an insight in the (periodic-cyclic) UWD pattern related to the temperature thresholds. These periodic patterns may be used for threshold-and/or seasonal dependent forecasting of UWD.

WT and Fourier analysis also detected 7-day UWD cycles, particularly in the more industrialized and larger city of Montreal (Fig. 4), which are related to fluctuations during the working week with 5-days work and 2-days off (Ruth et al. 2007). In the absence of a known natural forcing mechanism of a 7–8 day temperature cyclicity, the 7–8.5 day cycle between UWD and temperature could be related to an urban heating effect associated with the working week. For example, manufacturing industries with high energy requirements and heat outputs may increase the surrounding air temperature, and may lead to greater UWD, particularly in summer when UWD becomes very sensitive to air temperature. However, each city experiences different phase offsets between the 7-day UWD cycle and the 7-day temperature cycle. Therefore, a potential link between the 7-day UWD cycle related to the working week and a 7-day temperature cycle, such as a working week-related urban heating effect, appears to be elusive at this point. More detailed studies on the UWD heat island interaction may provide more evidence for the existence of such a link. For example, especially in the large manufacturing centers, the UWD and heating variability inside the city is high and can result in micro-climates where UWD interacts and responds in a very localized manner to meteorological changes. Studies could be set up to investigate the significance of such micro-climate interactions. Moreover, water resources managers could also benefit from the application of the wavelet analysis method to determine patterns and relationships on diurnal fluctuations that allow for short-time water supply and control adjustments.

7 Conclusion

Forecasting urban water demand is crucial in managing water demand and supply, particularly given the changes that will be incurred by climate change and population growth. Understanding associations between UWD and meteorological factors such as precipitation and air temperature can enable both better forecasting and a deeper understanding of the natural factors that drive urban water demand.

Wavelet analysis was investigated as a potential method for detecting patterns in UWD both in terms of the wavelength of cycles and the time of occurrence of these cycles, which is particularly useful as UWD varies according to season. The study demonstrated that CWT was able to detect cycles in UWD and meteorological factors, and their temporal range in a continuous scale-time resolution space. In contrast, DWT, which has been previously used for UWD forecasting (Adamowski et al. 2012), would not have been able to precisely detect most of the cycles illustrated in this study. For example, at a 1-day data interval record used for WT, DWT would

extract wavelet coefficients at a dyadic resolution such as for 2^8 days = 256 days and 2^9 days = 512 days, but not for the 365 days = 1 year cycle as was the case in this study.

When the CWT method was tested using data on UWD, air temperature and precipitation for Calgary, Montreal, and Ottawa, it was found that the annual (365 day) cycle dominated the air temperature and UWD patterns for all three cities studied. Fourier analysis was used to support the WT results, and detected a 7-day cycle in UWD in all three cities, which CWT had only detected in Montreal. This demonstrates the usefulness of using multiple approaches in studies such as this one.

A linear correlation between air temperature and UWD above a threshold of 10–12 °C was also identified. Given the strength of this correlation, applying seasonally dependent linear relationships between the UWD and temperature is suggested as perhaps more appropriate and potentially successful for forecasting than applying a continuous nonlinear function to explain all daily fluctuation throughout the entire record. The UWD–precipitation/temperature relationships in this study are derived from daily, and relatively short records, and do not reflect the long-term pattern. On multi-annual to centennial scale features such as population and economic growth, global warming, and fluctuations in oceanic-atmospheric circulation (House-Peters and Chang 2011; Ruth et al. 2007) superimpose the relationships found in this study that are based on daily to annual patterns.

Overall, this study found that WT is effective in detecting cycles in UWD and meteorological parameters, although Fourier analysis should be used in support of the results due to its more sophisticated detection of significance. Furthermore, the inclusion of projections based on linear correlations between air temperature and UWD under consideration of locally-dependent temperature thresholds could improve forecasting of UWD.

Acknowledgements This research was funded by a National Science and Engineering Research Council of Canada (NSERC) Grant and a Fonds de Recherche de Quebec—Nature et Technologies New Researcher Grant held by Jan Adamowski.

References

Adamowski J, Karapataki C (2008) Comparison of multivariate regression and artificial neural networks for peak urban water demand forecasting: the evaluation of different ANN learning algorithms. J Hydrol Eng 15(10):694–729. doi:10.1061/(ASCE)HE.1943-5584.0000245

Adamowski J, Chan HF, Prasher SO, Ozga-Zielinski B, Sliusarieva A (2012) Comparison of multiple linear and nonlinear regression, autoregressive integrated moving average, artificial neural network and wavelet artificial neural network methods for urban water demand forecasting in Montreal, Canada. Water Resour Res 48:W01528. doi:10.1029/2010WR009945

Adamowski K, Prokoph A, Adamowski J (2009) Development of a new method of wavelet aided trend detection and estimation. Hydrol Process 23:2686–2696. doi:10.1002/hyp.7260

Agthe DE, Billings RB (1980) Dynamic models of residential water demand. Water Resour Res 16(3):476–480. doi:10.1029/WR016i003p00476

Anderson R, Miller T, Washburn M (1980) Water savings from lawn watering restrictions during a drought year in Fort Collins, Colorado. J Amer Water Resour Ass 16(4):642–645. doi:10.1111/j.1752-1688.1980.tb02443.x

Arbués F, Barberán R, Villanúa I (2004) Price impact on urban residential water demand: a dynamic panel data approach. Water Resour Res 40:W11402. doi:10.1029/2004WR003092

Arbués F, Villanúa I, Barberán R (2010) Household size and residential water demand. Aust J Agric Resour Econ 54:61–80. doi:10.1111/j.1467-8489.2009.00479.x

Aubertin L, Aubin A, Pelletier G, Curodeau D, Osseyrane M, Lavallee P (2002) Identifying and prioritizing infrastructure rehabilitation. North American Society for Trenchless Technology, Liverpool

Bassett K, Tinline R (1970) Cross-Spectral analysis of time series and geographical research. Area 2:19–24

Coulibaly P (2006) Spatial and temporal variability of Canadian seasonal precipitation (1900–2000). Adv Water Resour 29:1846–1865. doi:10.1016/j.advwatres.2005.12.013

City of Calgary (2012) Calgary's water demand. www.calgary.ca/UEP/Water/Pages/Water-conservation/Calgarys-water-demand.aspx. Accessed 25th February 2012

City of Ottawa (2010) Water efficiency plan annual review 2010. Ottawa, ON

Davis JC (2002) Statistics and data analysis in geology, 3rd edn. Wiley, New York. 637 pp

Environment Canada (2010) Environmental trends. CESI 1 (3)

Environment Canada (2012) http://climate.weatheroffice.gc.ca/climateData/canada_e.html. Accessed 7th January 2012

Gato S, Jayasuriya N, Roberts P (2007) Temperature and rainfall thresholds for base use urban water demand modelling. J Hydrol 337(3–4):364–376. doi:10.1016/j.jhydrol.2007.02.014

House-Peters LA, Chang H (2011) Urban water demand modeling: review of concepts, methods, and organizing principles. Water Resour Res 47:W05401. doi:10.1029/2010WR009624

IPCC (2007) Climate change 2007: working group I report: the physical science basis. In: Solomon S, et al (eds) Fourth assessment report of the intergovernmental panel on climate change. Cambridge University Press, Cambridge, UK and New York, USA

Jenkins GM, Watts DG (1968) Spectral analysis and its applications. Holden-Day, New York

Maidment D, Parzen E (1984) Monthly water use and its relationship to climatic variables in Texas. Water Resour Bull 19(8):409–418

Maidment DR, Miaou SP (1986) Daily water use in nine cities. Water Resour Res 22(6):845–885. doi:10.1029/WR022i006p00845

Maidment D, Miaou S, Crawford M (1985) Transfer function models of daily urban water use. Water Resour Res 21(4):425–432. doi:10.1029/WR021i004p00425

Mann MS, Lees JM (1996) Robust estimation of background noise and signal detection in climatic time series. Clim Change 33:409–445. doi:10.1007/BF00142586

Maraun D, Kurths J (2004) Cross wavelet analysis: significance testing and pitfalls. Nonlinear Process Geophys 11:505–514. doi:10.5194/npg-11-505-2004

Maraun D, Kurths J, Holschneider M (2007) Nonstationary Gaussian processes in wavelet domain: synthesis, estimation, and significance testing. Phys Rev E 75:016707-1–13. doi:10.1103/PhysRevE.75.016707

Martínez-Espiñeira R (2002) Residential water demand in the northwest of Spain. Environ Resour Econ 21(2):161–187

Miaou SP (1990) A class of time series urban water demand models with nonlinear climatic effects. Water Resour Res 26(2):169–178. doi:10.1029/WR026i002p00169

Morlet J, Arehs G, Fourgeau I, Giard D (1982) Wave propagation and sampling theory. Geophysics 47:203–236.doi. doi:10.1190/1.1441328

Patterson RT, Prokoph A, Chang A (2004) Late Holocene sedimentary response to solar and cosmic ray activity influenced climate variability in the NE Pacific. Sediment Geol 172:67–84. doi:10.1016/j.sedgeo.2004.07.007

Praskievicz S, Chang H (2009) Identifying the relationships between urban water consumption and weather variables in Seoul, South Korea. Phys Geogr 30(4):324–337. doi:10.2747/0272-3646.30.4.324

Prokoph A, Barthelmes F (1996) Detection of nonstationarities in geological time series: wavelet transform of chaotic and cyclic sequences. Comput Geosci 22:1097–1108. doi:10.1016/S0098-3004(96)00054-4

Rioul O, Vetterli M (1991) Wavelets and signal processing. IEEE Signal Process Mag 8(4):14–38. doi:10.1109/79.91217

Ruth M, Bernier C, Jollands N, Golubiewski N (2007) Adaptation of urban water supply infrastructure to impacts from climate and socioeconomic changes: the case of Hamilton, New Zealand. Water Res Man 21:1031–1045. doi:10.1007/s11269-006-9071-x

Schaefli B, Maraun D, Holschneider M (2007) What drives high flow events in the Swiss Alps? Recent developments in wavelet spectral analysis and their application to hydrology. Adv Water Resour 30:2511–2525. doi:10.1016/j.advwatres.2007.06.004

Schleich J, Hillenbrand T (2009) Determinants of residential water demand in Germany. Ecol Econ 68:1756–1769. doi:10.1016/j.ecolecon.2008.11.012

Schulz M, Mudelsee M (2002) REDFIT: estimating red-noise spectra directly from unevenly spaced paleoclimatic time series. Comput Geosci 28:421–426. doi:10.1016/S0098-3004(01)00044-9

Torrence C, Compo GP (1998) A practical guide to wavelet analysis. Bull Am Meteorol Soc 79:61–78. doi:10.1175/1520-0477(1998)079<0061:APGTWA>2.0.CO;2

Ware DM, Thomson RE (2000) Interannual to multidecadal timescale climate variations in the Northeast Pacific. J Climate 13:3209–3220. doi:10.1175/1520-0442(2000)013<3209:ITMTCV>2.0.CO;2

Zhang X, Vincent A, Hogg WD, Niitsoo A (2000) Temperature and precipitation trends in Canada during the 20th century. Atmos-Ocean 38:395–429. doi:10.1080/07055900.2000.9649654

Zhou S, McMahon T, Walton A, Lewis J (2000) Forecasting daily urban water demand: a case study of Melbourne. J Hydrol 236:153–164. doi:10.1016/S0022-1694(00)00287-0